



PAPER • OPEN ACCESS

## Effect of potassium on structural, photocatalytic and antibacterial activities of ZnO nanoparticles

To cite this article: R Bhaviya Raj *et al* 2016 *Adv. Nat. Sci: Nanosci. Nanotechnol.* **7** 045008

View the [article online](#) for updates and enhancements.

### You may also like

- [The Dependence of Crystal Plane on Hydrogen Sensing Properties of ZnO Bulk Substrates](#)  
Soohwan Jang, Sunwoo Jung and Kwang Hyeon Baik
- [Electronic properties of graphene-ZnO interface: a density functional theory investigation](#)  
Maryam Fathzadeh, Hamoon Fahravandi and Ebrahim Nadimi
- [Doping dependence of the surface phase stability of polar O-terminated \(0001\) ZnO](#)  
Simon Erker, Patrick Rinke, Nikolaj Moll et al.

# Effect of potassium on structural, photocatalytic and antibacterial activities of ZnO nanoparticles

R Bhaviya Raj, M Umadevi, V Poornima Parvathi and R Parimaladevi

Department of Physics, Mother Teresa Women's University, Kodaikanal—624102, India

E-mail: [ums10@yahoo.com](mailto:ums10@yahoo.com)

Received 8 August 2016

Accepted for publication 20 September 2016

Published 13 October 2016



## Abstract

ZnO and potassium doped ZnO nanoparticles were synthesized through wet chemical method. The samples were characterized by UV, XRD, SEM, TEM and EDAX. XRD analysis reveals that the prepared nanoparticles exhibit hexagonal wurtzite structure. TEM and SEM analyses disclose that synthesized samples were porous structure with needle shape. It also confirms that potassium was dispersed on ZnO surface. The influence of potassium on ZnO surface modulates the degradation of textile dyeing wastewater by improving its rate of decomposition to  $0.007 \text{ min}^{-1}$  with decoloration. A better zone of inhibition of about 20 mm against *Staphylococci aureus* and *Pseudomonas aeruginosa* by ZnO and potassium doped ZnO nanoparticles were measured. The findings suggest that these nanoparticles have the potential to be a good photocatalyst and applied in water treatment to inhibit the bacterial growth.

Keywords: antibacterial activity, photocatalytic activity, TEM, XRD, ZnO

Classification numbers: 2.00, 4.00, 4.04, 5.01, 5.07

## 1. Introduction

Waste water from the textile industry is a complex and highly variable mixture of many polluting substances ranging from inorganic compounds and elements to polymers and organic products [1]. Due to the aesthetically improper color and toxicity of textile dye waste water it contributes to water pollution and troubles aquatic flora/fauna and also human beings [2]. Hence the removal of the finest contaminants from dyeing waste water is needed. Metal nanoparticles with antimicrobial activity when embedded and coated on to surfaces can find immense applications in water treatment, synthetic textiles, biomedical and surgical devices, food processing and packaging [3]. One of the most important and surface-dependant properties of ZnO nanoparticles is their photocatalytic behavior under UV electromagnetic irradiation. This behavior can be used for degradation and removal of

environmental pollutants, especially organic dye contaminants, from water [4].

Photocatalysis is a promising technique for solving many current environmental and energy issues [5]. The most intensively used species in photocatalyst is the zinc oxide due to its advantage of low cost and more active catalyst than  $\text{TiO}_2$  in photodegradation process [6]. Differently shaped ZnO nanoparticles such as spherical [4], flower-like [7], tetrapod [8], sheets [9], flakes [10] etc can be synthesized. Hoffman *et al* have observed the production of  $\text{H}_2\text{O}_2$  on ZnO as early as 1994 [11]. Nguyen *et al* [12] synthesized ZnO nanoplates decorated by  $\text{WO}_3$  nanorods by hydrothermal method for  $\text{NH}_3$  gas sensing application. It has also observed that green synthesized ZnO nanoparticles acted as a proficient photocatalyst in removal of anthracene [13], reactive blue 198 (RB 198) and dye from real textile dyeing wastewater [14]. The nature, morphology, concentration, and state of the catalyst material, also, have a great influence on the microbial inactivation rates [15]. Illuminated ZnO material with ultra-violet (UV) light can generates electron/hole pairs. These electrons and holes can migrate and initiate redox reactions with water and oxygen, by which they degrade organic



Original content from this work may be used under the terms of the Creative Commons Attribution 3.0 licence. Any further distribution of this work must maintain attribution to the author(s) and the title of the work, journal citation and DOI.

molecules adsorbed on the surface of a photocatalyst [16]. ZnO is an environmentally friendly material, high chemical stability and low toxicity, and is widely used as an active ingredient for dermatological applications in creams, lotions and ointments on an account of its antibacterial properties [17]. Doping is an effective and facile method to improve the photocatalytic properties of ZnO by boosting the absorption of light. Incorporation of dopant ions is able to generate lattice defects and variation of band gap energy [18]. Potassium chloride is highly soluble, and readily undergoes dissociation.

In this paper ZnO (Z) and potassium doped ZnO nanoparticles (PZ) nanoparticles were synthesized by wet chemical method. Hexagonal wurtzite structure of ZnO was evident from x-ray diffraction (XRD) analysis. The presence of ZnO was confirmed in Fourier transform infrared spectroscopy (FTIR) spectra. Needle like morphology and porous nature was evident through scanning electron microscopy (SEM) and transmission electron microscopy (TEM). PZ showed higher rate of decomposition of  $0.007 \text{ min}^{-1}$  with textile dye waste water and better zone of inhibition against *S. aureus* and *P. aeruginosa*.

## 2. Experimental

### 2.1. Materials

Zinc chloride ( $\text{ZnCl}_2$ ), sodium hydroxide (NaOH), potassium chloride (KCl) and spectral grade ethanol was purchased from NICE. All the chemicals were of analytical grade and used as purchased without further purification. Doubly distilled water was used throughout the experiment. Dyed waste water was collected from the textile dyeing industry of Tamil Nadu.

### 2.2. Synthesis of Z and PZ nanoparticles

Synthesis procedure of Z and PZ was done as in literature [19] with slight modifications. 1 M solution of  $\text{ZnCl}_2$  and 1 M of NaOH in 100 ml and 250 ml of distilled water were stirred separately in a magnetic stirrer for about 45 min each. These solutions were then mixed together and stirred in the magnetic stirrer for an hour and the mixture was allowed to sediment for 5 h. The deposited substance was then washed with distilled water and ethanol to remove the impurities to the possible extent. The paste was dried on a hot plate at  $80^\circ\text{C}$  and the resultant white solid product was allowed to cool at room temperature and crushed into powder in agate mortar pestle. The powder was coded as Z. Potassium doped zinc oxide was prepared by adding 0.1 g of potassium chloride to 1 M of zinc chloride in 100 ml of distilled water and the above mentioned procedure was repeated and the powder was coded as PZ.

### 2.3. Characterization

The UV-vis absorption spectra of the Z and PZ nanoparticles were recorded by Shimadzu UV 2600 in a diffuse reflectance mode using  $\text{BaSO}_4$  as reference, and Shimadzu UV 1700 was used to record the absorption spectra of textile dyeing wastewater (TWW), textile dyeing wastewater with pure zinc

oxide (TWW + Z) and textile dyeing wastewater with potassium doped zinc oxide (TWW + PZ) using distilled water as reference. The XRD analysis was carried out on Burker advanced x-ray diffractometer using  $\text{Cu-K}\alpha$  radiation ( $\lambda = 1.5406 \text{ \AA}$ ) in a  $2\theta$  diffraction interval of  $30^\circ$ – $80^\circ$ . FTIR measurements were obtained on Perkin Elmer FTIR spectrometer using KBr pellets. The morphological characterization was carried out by SEM observation using FEI Quanta200, Czechoslovakia equipped with energy dispersive analysis of x-rays (EDAX). The TEM investigations were performed by JEOL TEM 2100, operating at 200 kV.

### 2.4. Photocatalytic activity

The photocatalytic efficiency of Z and PZ were evaluated by the rate of decomposition and decolorization of TWW under UV light irradiation. In this experiment, 10 mL of TWW (in 30 ml distilled water) was added in 0.17 g of Z (in 25 ml distilled water). The test was performed by irradiating the nanoparticle under ultraviolet light at an interval of 10 min and the absorbance changes of TWW were studied.

### 2.5. Antimicrobial studies

The antimicrobial activity of Z and PZ was evaluated against gram negative *P. aeruginosa* and gram positive *S. aureus* (MTCC-7443) by disc diffusion method. 0.5 ml of fresh cultures of each organism was inoculated into 5 mL of sterile nutrient broth (Hi Media) and incubated at  $37^\circ\text{C}$  for 24 h to standardize the culture. These culture media were prepared by spreading  $100 \mu\text{l}$  of the revived culture on MHA (Mueller Hinton Agar-Hi Media). The well was made having a diameter of 5 mm and  $100 \mu\text{l}$  samples of Z and PZ were added in the well and  $30 \mu\text{l}$  of dimethyl sulfoxide (DMSO) as a control. The petri plates were kept at  $37^\circ\text{C}$  for 24 h in an incubator for microorganisms during which its antibacterial activity was evidenced by the presence of a zone of inhibition (mm) surrounding the well.

## 3. Results and discussion

### 3.1. Optical and vibrational studies

The ZnO have direct narrow band gap. Figure 1(a) shows the UV-visible spectra of Z and PZ nanoparticles. Tauc plot was employed to find the energy band gap of the nanoparticles. The energy band gap ( $E_g$ ) [20] of Z nanoparticles was found to be 3.23 eV, whereas the  $E_g$  for PZ was determined as 3.25 eV (figure 1(b)). The experimental results indicates that the band gap energies of ZnO and K doped ZnO nanoparticles were not changed, that is to say, K doping does not play an important role in optical band gap of ZnO nanoparticles.

Figure 1(c) shows the FTIR spectra of Z and PZ nanoparticles. In the spectra, the bands in the region  $579 \text{ cm}^{-1}$  and  $447 \text{ cm}^{-1}$  of Z and  $569 \text{ cm}^{-1}$  and  $458 \text{ cm}^{-1}$  of PZ represent the stretching mode of Zn–O [21]. The band in the region  $3100$ – $3400 \text{ cm}^{-1}$  corresponds to the O–H stretching vibration which is due to the absorption of water molecules during

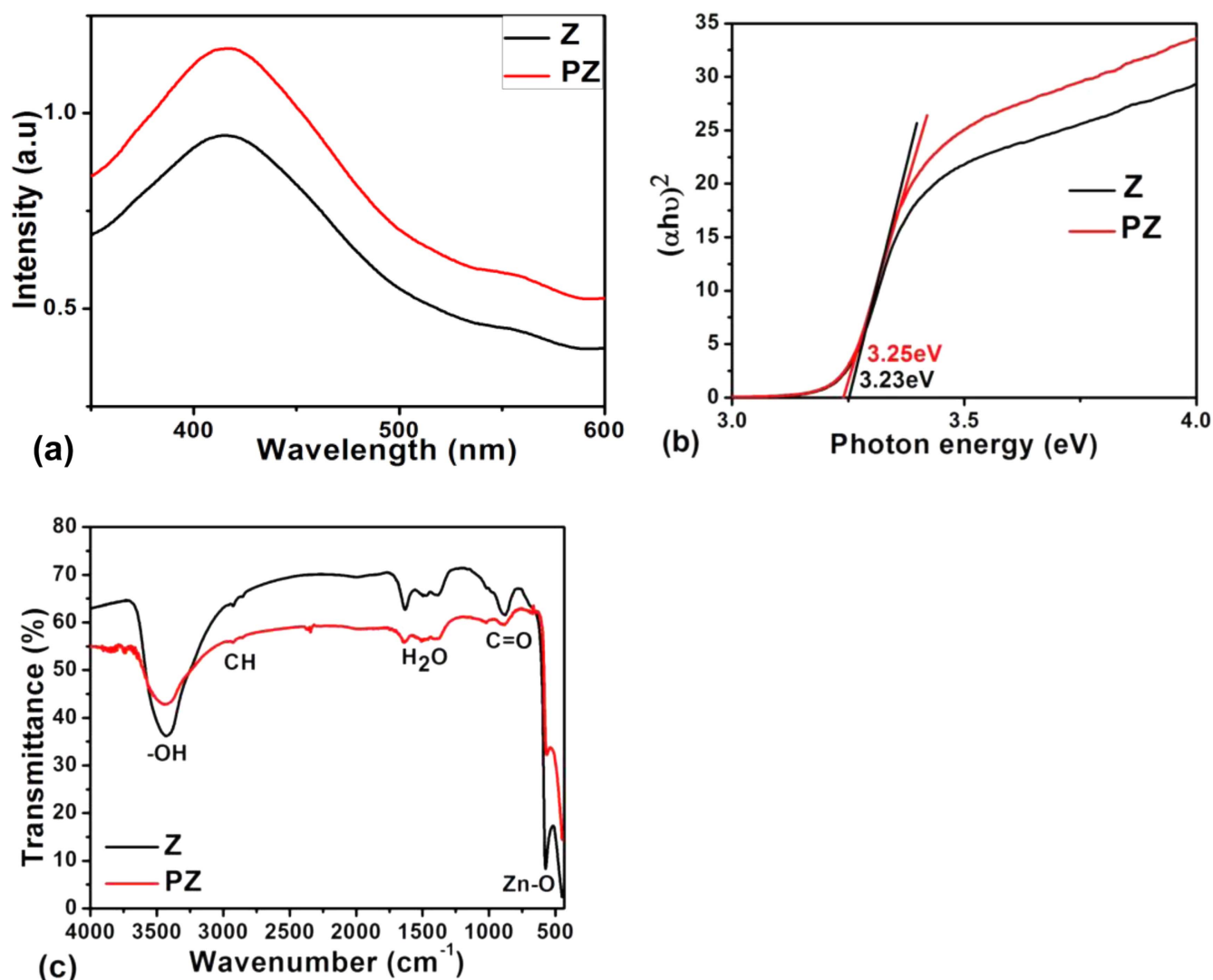


**Figure 1.** (a) UV-vis spectra, (b) energy band gap and (c) FTIR spectra of Z and PZ nanoparticles.

the process of recording FTIR spectra. The bands in the region of 1300–3000  $\text{cm}^{-1}$  correspond to the C–H stretching vibration. The physisorbed H<sub>2</sub>O molecules on particle surface and C=O stretching vibrations were observed at 1635  $\text{cm}^{-1}$ , 1638  $\text{cm}^{-1}$  and 800–900  $\text{cm}^{-1}$ , respectively. The strong absorption band of hydroxyl group of PZ indicates hydrogen bond formed at ZnO/K interface. This indicates that the concentrations of surface hydroxyl group are related to potassium dopant, which affects the photocatalytic activity.

### 3.2. Structural and morphological studies

The XRD analysis was carried out for the synthesized samples (figure 2(a)). The peaks are characteristics of zinc oxide (JCPDS no. 891397) with hexagonal wurtzite structure with preferred orientation along the (101) direction. The broad peaks are due to the small particle size of the prepared sample and its sharpness indicates that the product is crystalline in nature. When comparing with the diffraction peaks of Z and PZ samples, no characteristics peaks of dopant K and other phases such as Zn(OH)<sub>2</sub> and KOH on ZnO photocatalyst

suggested that K nanoparticles did not influence the structure. Thus K was not incorporated into the lattice of ZnO and it was merely deposited on the surface of catalyst.

The SEM images depicted in (i) and (ii) of figure 2(b) show that shape of Z and PZ represent ‘needle-like’ agglomerates with less porous structure. The same morphology is observed in the TEM images of the nanoparticles (figure 2(b): (iii) and (iv)). Thus K doping does not change the morphology markedly, however small K particles appear on ZnO surface. SEM and TEM picture of Z and PZ depicts that nanoparticles are porous in nature. Porous and hollow structured ZnO is impressive because of its nanostructured wall, hollow interior, large specific area, low density and good surface permeability. Therefore porous and hollow nature of ZnO provides feasible platforms to achieve improved performance of devices and enhanced catalytic activity for organic pollutant transport. The elemental microanalysis of PZ shows (figure 2(c)) the composition of Zn (65.9%), O (33.5%) and K (0.6%) in weight%, which confirms the presence of potassium in ZnO nanostructure. The inset in figure 2(c) shows the dispersion of K on the surface of ZnO.

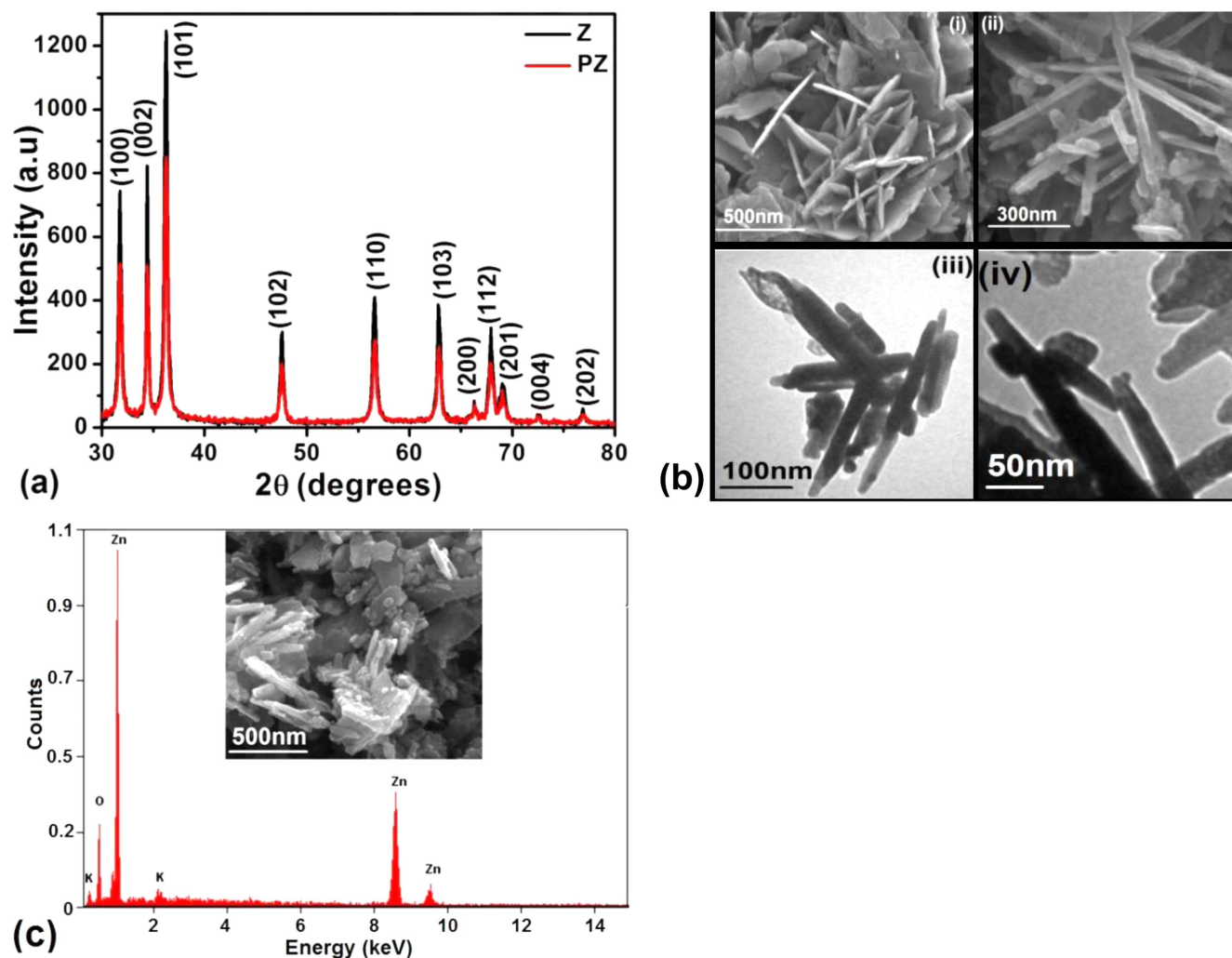
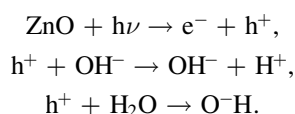


**Figure 2.** (a) XRD pattern of Z and PZ nanoparticles; (b): (i) and (ii) are the SEM images of Z and PZ, respectively, and (iii) and (iv) are the TEM images of Z and PZ nanoparticles respectively; (c) energy dispersive x-ray analysis (EDAX) of PZ nanoparticle.

### 3.3. Applications

**3.3.1. Photocatalytic activity.** The semiconductor catalysts promote photocatalytic reactions under the illumination of UV radiation [21]. ZnO is used for photocatalytic oxidation of several pollutants as their photocatalytic ability can exploit antimicrobial coatings and allow thin coatings to be self cleaning and to have disinfecting properties after exposure to UV radiation. Electrons in the semiconductor are excited from the valence band to the conduction band leaving positive holes in the valence band. The electrons in the conduction band react with the adsorbed oxygen molecules to form  $O^{2-}$  species, while the positive holes react with the adsorbed hydroxyl ions to form hydroxyl radicals. The possible route of hydroxyl free radical formation is shown here [22]:



From the time dependent absorbance spectra figure (a), (b) and (c) of the textile dye solution, it is obvious that the

absorbance peak at 410 nm is reduced significantly, thus indicating the degradation of the dye molecules. After 120 min PZ shows complete decoloration of textile dye and Z shows less decoloration ability, while pure dye textile almost does not decolorize. The K on ZnO surface leads to the further separation of photogenerated electrons and holes which leads to production of hydroxide ( $\text{OH}^\cdot$ ) and superoxide ( $\text{O}^{2-}$ ) radicals. As a result, the photocatalytic activity of ZnO is further enhanced which is attributed to abundant surface hydroxyl and superoxide groups on K/ZnO photocatalysts which also confirms by FTIR studies. A good linear correlation of rate constants were estimated quantitatively to be  $0.0001 \text{ min}^{-1}$ ,  $0.005 \text{ min}^{-1}$  and  $0.007 \text{ min}^{-1}$  (figure 3(d)) for the samples TWW, TWW + Z and TWW + PZ, respectively, by the pseudo-first order reaction [23] between the plot of  $\ln(C_t/C_0)$  versus time. The results revealed that TWW + PZ photocatalyst exhibited the highest  $K_{\text{app}}$  value compared to Z. Potassium on ZnO surface act as electron sink, promote interfacial charge transfer kinetics between potassium and ZnO reduce the recombination of photo induced electrons in the conduction band and holes in the



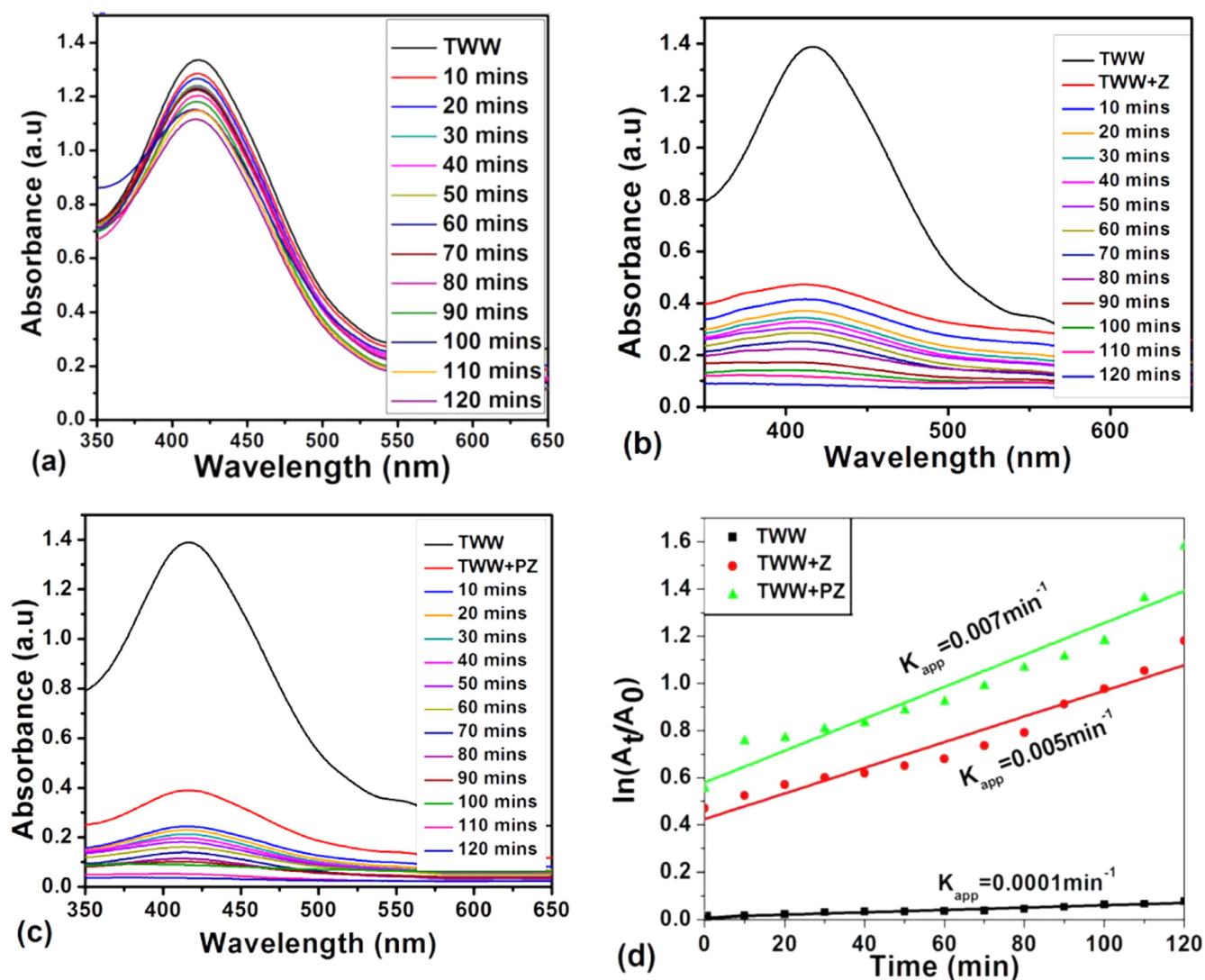


**Figure 3.** (a)–(c) Degradation graph of TWW, TWW + Z and TWW + PZ, respectively; and (d) rate of decomposition of TWW, TWW + Z and TWW + PZ.

valence band and extend the life time of the electron-hole pairs, thus increasing the photocatalytic activity of K/ZnO photocatalyst. Moreover the hexagonal shape of the nanoparticles might be the reason for higher degradation efficiency.

**3.3.2. Antibacterial activity.** The ZnO nanoparticles have selective toxicity to bacteria and only exhibit minimal effect on human cells, which recommend their prospective uses in agricultural and food industries [24]. Zinc ions are known to inhibit multiple activities in the bacterial cell, such as glycolysis, transmembrane proton translocation, and acid tolerance [25]. In this work the antibacterial activity of Z and PZ nanoparticles was performed against gram negative pathogen *P. aeruginosa* and gram positive pathogen *S. aureus* which are commonly found in water. The effect of antibacterial activity was more pronounced in *S. aureus* in Z (figure 4(a)) and *P. aeruginosa* in PZ with its zone of inhibition of about 20 mm. Antibacterial activity of Z and PZ

nanoparticles against two different pathogens are represented in figure 4(b). Concentration of 100  $\mu\text{l}$  of Z and PZ nanoparticles showed bacteriostatic affect against both the pathogens and retarded the growth of both pathogens. Z and PZ continuously interact with the bacterial cells and thus, they exhibit excellent toxicity against *P. aeruginosa* and *S. aureus* bacteria. Gram negative bacteria, *P. aeruginosa* exhibit only a thin peptidoglycon layer between the cytoplasmic membrane and outer membrane. When Z particles dispersed in the growth media  $\text{Zn}^{2+}$  present in ZnO interacted with bacterial cells and adheres to the bacterial cell walls. The overall charge on bacterial cell surface at biological pH values is negative, which is due to the excess number of carboxylic and other groups that upon dissociation make the cell surface negative [26]. The adhesion and bio activity may due to bacteria and  $\text{Zn}^{2+}$  atoms. The zinc shows variable activity on the species. However, *S. aureus* shows more sensitive towards Z nanoparticle than *P. aeruginosa* [27]. This is due to polarity of their cell membrane. Sonahare *et al* [28] reported that *S. aureus* membrane has a smaller negative level

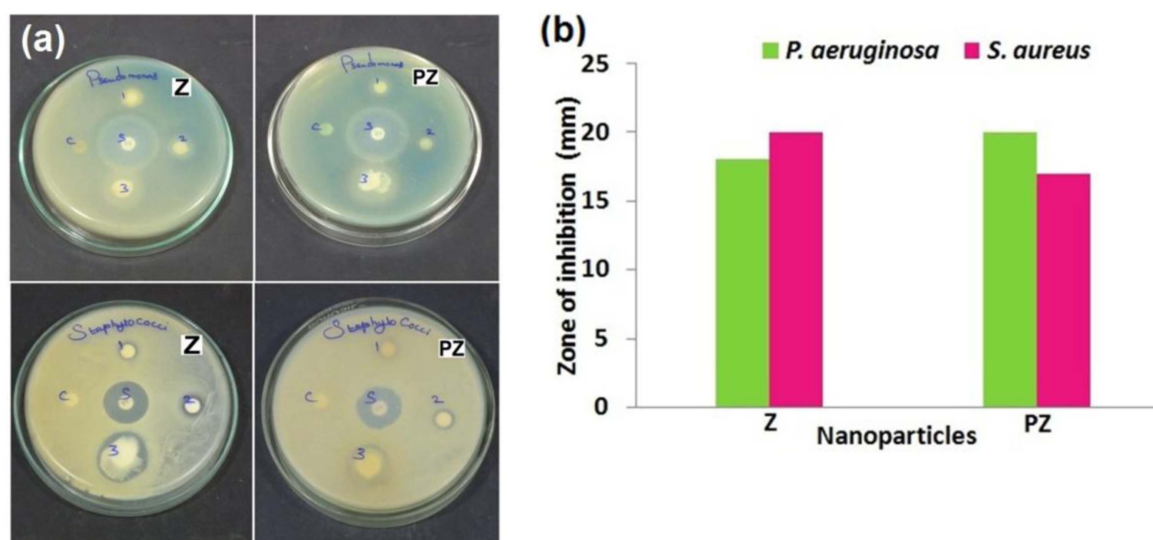


**Figure 4.** (a) Zone of inhibition of Z and PZ nanoparticles on *P. aeruginosa* and *S. aureus*, (b) antibacterial activity of Z and PZ against two different bacteria.

of penetration of negative charged free radicals such as superoxide radical anions and peroxide ions, causing damage and cell death to *S. aureus* than required for *P. aeruginosa*.

#### 4. Conclusion

In summary, potassium dispersed ZnO nanoparticles were successfully prepared by wet chemical method. The samples exhibited hexagonal wurtzite structure. Structural and morphological analysis confirms porous and hollow nature of ZnO, which provides feasible platforms to achieve improved performance of devices and enhanced catalytic activity for organic pollutant transport. The positive effect on photo-degradation of textile dye water was due to trapping of photo induced electrons and holes to form more active hydroxyl radicals. Further the presence of potassium on surface of ZnO reduces the recombination of light generated electron-hole pair at ZnO surface and enhances the photocatalytic efficiency of ZnO. The zone of inhibition was observed against pathogenic bacteria suggests that the PZ nanoparticles exhibit excellent antibacterial activity. Therefore the PZ nanoparticles have efficient potential to be applied in the process of treating dyeing wastewater from the textile industries and can be used in bacterial treatment. This work has resulted in an effective way of decoloration of wastewater from the textile dyeing industry. The development of such compound as heterogeneous photocatalyst used as immobilized photocatalysts for water and environment detoxification from organic and inorganic compounds like arsenic and bacteria.

#### Acknowledgments

This work was partially funded by DST-CURIE, Grant No. SR/CURIE/02/ 2010, New Delhi.

#### References

- [1] Banat I M, Nigam P, Singh D and Marchant R 1996 *Bioresour. Technol.* **58** 217
- [2] Lade H S, Waghmode T R, Kadam A A and Govindwar S P 2012 *Int. Biodeterior. Biodegrad.* **72** 94
- [3] Gutierrez F M, Olive P L, Banuelos A, Orrantia E, Nino N, Sanchez E M, Ruiz F, Bach H and Av-Gay Y 2010 *Nanomedicine* **6** 681
- [4] Ali O and Rahimeh N 2012 *Res. Chem. Intermed.* **38** 323
- [5] Ravelli D, Dondi D, Fagnoni M and Albini A 2009 *Chem. Soc. Rev.* **38** 1999
- [6] Hoffman A J, Carraway E R and Hoffmann M R 1994 *Environ. Sci. Technol.* **28** 776
- [7] Duo S, Li Y, Zhang H, Liu T, Wu K and Li Z 2016 *Mater. Charact.* **114** 185
- [8] Modi G 2015 *Adv. Nat. Sci.: Nanosci. Nanotechnol.* **6** 033002
- [9] Xiao Q, Huang S, Zhang J, Xiao C and Tan X 2008 *J. Alloys Compd.* **459** L18
- [10] Bouvy C, Marine W and Su B L 2007 *Chem. Phys. Lett.* **438** 67
- [11] Wang Z L 2004 *Mater. Today* **7** 26
- [12] Nguyen D D, Do D T, Vu X H, Dang D V and Nguyen D C 2016 *Adv. Nat. Sci.: Nanosci. Nanotechnol.* **7** 015004
- [13] Hassan S S M, Azab W I M E, Ali H R and Mansour M S M 2015 *Adv. Nat. Sci.: Nanosci. Nanotechnol.* **6** 045012
- [14] Nguyen V C, Nguyen N L G and Pho Q H 2015 *Adv. Nat. Sci.: Nanosci. Nanotechnol.* **6** 035001
- [15] Baruah S, Pal S K and Dutta J 2012 *Nanosci. Nanotechnol. Asia* **2** 90
- [16] Bourfaa F, Lamri Zeggag M, Adjimi A, Aida M S and Attaf N 2016 *IOP Conf. Series: Mater. Sci. Engg.* **108** 012049
- [17] Sankara Reddy B, Venkatramana Reddy S, Koteeswara Reddy N and Pramoda Kumari J 2013 *Research J. Mater. Sci.* **1** 11
- [18] Sakthivel S, Neppolian B, Shankar M V, Arabinthoo B, Palanichamy M and Murugesan V 2003 *Sol. Energ. Mat. Sol. C* **77** 65
- [19] Awodugba A O and Ilyas A-M O 2013 *Asian J. Nat. Appl. Sci.* **2** 41
- [20] Sasi Florence S, Umadevi M, John R, Sindhu Kumari B and Lawrence Arockiasamy D 2013 *Mater. Lett.* **108** 5

- [21] Sung-Suh H M, Choi J R, Hah H J, Koo S M and Bae Y C 2004 *J Photochem, Photobiol. A* **163** 37
- [22] Karimi L and Zohoori S 2013 *J. Nanostructure Chem.* **3** 32
- [23] Umadevi M, Parimaladevi R and Sangari M 2014 *Spectrochim. Acta Part A: Molecular and Biomolecular Spectroscopy* **120** 365
- [24] Zhang L L, Jiang Y H, Ding Y L, Povey M and York D 2007 *J. Nanopart. Res.* **9** 479
- [25] Phan T N, Buckner T, Sheng J, Baldeck J D and Marquis R E 2004 *Oral Microbiol. Immunol.* **19** 31
- [26] Amna T, Hassan M S, Barakat N A M, Pandiya D R, Hong S T, Khil M S and Kim H Y 2012 *Appl. Microbial Biotechnol.* **93** 743
- [27] Reddy K M, Feris K, Bell J, Wingett D G, Hanley C and Punnoose A 2007 *Appl. Phys. Lett.* **90** 1
- [28] Sonohara R, Muramatsu N, Ohshima H and Konda T 1995 *Biophys. Chem.* **55** 273